# A Single Intravitreal Injection of Ranibizumab Provides No Neuroprotection in a Nonhuman Primate Model of Moderate-to-Severe Nonarteritic Anterior Ischemic Optic Neuropathy

Neil R. Miller,[1,2] Mary A. Johnson,[2] Theresa Nolan,[3] Yan Guo,[2] and Steven L. Bernstein[2]

[1]The Wilmer Eye Institute, the Johns Hopkins Medical Institutions, Baltimore, Maryland, United States
[2]Department of Ophthalmology and Visual Sciences, the University of Maryland School of Medicine, Baltimore, Maryland, United States
[3]Department of Veterinary Resources, the University of Maryland School of Medicine, Baltimore, Maryland, United States

Correspondence: Neil R. Miller, Woods 458, Wilmer Eye Institute, Johns Hopkins Hospital, 600 North Wolfe Street, Baltimore, MD 21287, USA;
nrmiller@jhmi.edu.

Submitted: August 21, 2015
Accepted: October 19, 2015

Citation: Miller NR, Johnson MA, Nolan T, Guo Y, Bernstein SL. A single intravitreal injection of ranibizumab provides no neuroprotection in a nonhuman primate model of moderate-to-severe nonarteritic anterior ischemic optic neuropathy. *Invest Ophthalmol Vis Sci*. 2015;56:7679–7686. DOI:10.1167/iovs.15-18015

**Purpose.** Ranibizumab, a vascular endothelial growth factor-antagonist, is said to be neuroprotective when injected intravitreally in patients with nonarteritic anterior ischemic optic neuropathy (NAION). We evaluated the efficacy of a single intravitreal (IVT) injection of ranibizumab in a nonhuman primate model of NAION (pNAION).

**Methods.** We induced pNAION in one eye of four adult male rhesus monkeys using a laser-activated rose Bengal induction method. We then immediately injected the eye with either ranibizumab or normal saline (NS) intravitreally. We performed a clinical assessment, optical coherence tomography, electrophysiological testing, fundus photography, and fluorescein angiography in three of the animals (one animal developed significant retinal hemorrhages and, therefore, could not be analyzed completely) prior to induction, 1 day and 1, 2, and 4 weeks thereafter. Following the 4-week analysis of the first eye, we induced pNAION in the contralateral eye and then injected either ranibizumab or NS, whichever substance had not been injected in the first eye. We euthanized all animals 5 to 12 weeks after the final assessment of the second eye and performed both immunohistochemical and light and electron microscopic analyses of the retina and optic nerves of both eyes.

**Results.** A single IVT dose of ranibizumab administered immediately after induction of pNAION resulted in no significant reduction of clinical, electrophysiological, or histologic damage compared with vehicle-injected eyes.

**Conclusions.** A single IVT dose of ranibizumab is not neuroprotective when administered immediately after induction of pNAION.

Keywords: anterior ischemic optic neuropathy, ranibizumab, intravitreal injection, neuroprotection

Nonarteritic anterior ischemic optic neuropathy (NAION) is caused by inadequate blood supply to the optic nerve head (i.e., the optic disc) and is the leading cause of sudden optic nerve-related vision loss in individuals over 50 years old.[1] In the United States, it affects 2.3 to 10.2 per 100,000 people over 50 years of age,[2,3] resulting in over 10,000 new cases per year. Very little is understood concerning the pathophysiology of the disease, and there currently is no medical or surgical treatment that has been proven to be consistently beneficial.[4]

We have developed reproducible rodent and nonhuman primate models of NAION (rNAION, pNAION) using an intravenous (IV) injection of rose Bengal (RB) followed by intraocular laser photoactivation of the dye at the optic nerve head (ONH). This technique produces an optic neuropathy that, despite having a different etiology, clinically, electrophysiologically, and histopathologically resembles human NAION.[5–8] These models provide an invaluable resource because they can be used to analyze critically the mechanisms resulting in post ischemic ON damage, and because they can be used as tools in the evaluation of potential neuroprotective and neuroreparative therapies for patients who experience NAION.

One of the many treatments suggested to improve visual outcome in patients with NAION is IVT injection of one of the VEGF antagonists. For example, Bennett et al.[9] reported a small series of patients in whom treatment of acute NAION with a single IVT injection of 1.25 mg of the anti-VEGF agent bevacizumab was associated with an improved visual outcome; however, a small nonrandomized prospective trial (17 patients treated; 8 patients not treated) using the same treatment failed to show any benefit in visual outcome or peripapillary retinal nerve fiber layer (PRNFL) thickness (as assessed using optical coherence tomography [OCT]) between treated and non-treated subjects.[10] In addition, Huang et al.[11] reported no beneficial effect of IVT ranibizumab in adult rats with laser-induced AION as assessed by measurements of retinal ganglion cell (RGC) densities, flash-evoked VEP latencies and amplitudes, number of apoptotic cells in the RGC layer, and ED1-positive cells per high-power field. Not only may IVT injections of anti-VEGF agents be nontherapeutic, they may cause harm.

Several cases have been reported in which the development of NAION was related temporally to an IVT injection of an anti-VEGF agent for AMD.[12,13] In light of this controversy, we elected to test the efficacy of ranibizumab (Lucentis; Genentech, San Francisco, CA, USA) in our pNAION model.

## Methods

### Animals

All animal protocols were approved by the University of Maryland Institutional Animal Care and Utilization Committee (IACUC; Baltimore, MD, USA) and adhered to the ARVO Statement for the Use of Animals in Ophthalmic and Vision Research. For induction of pNAION, four male rhesus monkeys (*Maccaca mulatta*, age 4–6 years, 6–14 kg) were anesthetized with a mixture of ketamine (10 mg/kg) and xylazine (2 mg/kg). For subsequent assessments, the animals were anesthetized initially with intramuscular (IM) ketamine, followed by an intramuscular injection of atropine to reduce oral secretions. After initial anesthetization, a pupillary examination, including testing of the pupillary light reflex and a swinging flashlight test to determine if a relative afferent defect (RAPD) was present, was performed. The animals then were intubated, and further assessments performed while the animals were supported with a continuous infusion of propofol. Propofol was used because it does not suppress cortical electrical responsiveness.[14] Intermittent IV or IM injections of ketamine were used throughout the assessment to reduce spontaneous eye movements.

### pNAIon Induction

We induced pNAION in four animals (A1, J1, O1, and S1) for our studies. Although pNAION was induced in both eyes of all four animals, the inductions were sequential, not simultaneous, with the second eye induced 5 weeks after the first eye. The procedure for induction of pNAION has been described previously.[8] Briefly, after anesthetization with ketamine and xylazine, the pupil of one of the monkey's eyes was dilated with a combination of 1% tropicamide and 2.5% phenylephrine. The animal then was placed in front of a slit-lamp biomicroscope fitted with an ophthalmic neodymium-yttrium-aluminum-garnet (Nd-YAG) frequency-doubled diode laser (532 nm: Iridex, Mountain View, CA, USA). For pNAION induction, we replaced the 209-μm diameter laser fiberoptic cable with a 500-μm diameter fiberoptic cable that had SMA adapter ends. This alteration enabled us to use the standard 532-nm slit-lamp adapter to generate a 1.06-mm spot size using the 200-μm spot size setting. The optic disk in the eye to be lasered was visualized using a Glasser monkey contact lens (Ocular Instruments, Inc., Bellevue, WA, USA), and pNAION was induced by injecting RB IV in a dose of 2.5 mg/kg of lean body weight, followed 30 seconds later by dye activation at the optic disk using the 1.06-mm spot size, at 200mW, for times ranging from 8.5 to 9 seconds. These parameters were chosen to produce a moderate-to-serve optic neuropathy (i.e., the severity that would be most likely to warrant treatment in a patient with human NAION). With equivalent induction times, laser power and dye administration, the generated lesion was consistent between eyes of a given animal. Thus, we were able to produce similar damage in the optic nerves of each animal that enabled us to use one eye as a vehicle control, and the other for ranibizumab treatment. Regardless of the severity of damage, all animals had preserved visual function after each induction, as assessed by overall behavior, pupillary responses to light stimulation, and electrophysiologic assessment. Thus, despite being visually impaired from pNAION induction in both eyes, the animals were not blinded during the course of this study. This approach considerably reduced the total number of animals needed for the study and enabled us to compare directly responses between eyes of the same animal.

### Neuroprotection Experiments

**Intravitreal Injection.** Eyes were injected with ranibizumab or normal saline (NS) immediately after pNAION induction. Prior to injection, eyes were prepped three times with 5% povidone iodine and anesthetized with viscous ophthalmic tetracaine (Tetravisc; OCuSOFT, Rosenberg, TX, USA). Topical ciprofloxacin drops were instilled and the induced eye received an IVT injection consisting of either 0.05 mL of sterile filtered saline (vehicle; J1, O1) or a 0.05 mL solution containing 0.5 mg of sterile filtered ranibizumab (A1, S1). The dose of ranibizumab was chosen because it is the maximum dose injected in humans for a variety of ocular conditions such as wet AMD and diabetic maculopathy,[15,16] and because of the size of the adult rhesus eye relative to the adult human eye.[17] Five to 8 weeks following pNAION induction and injection of the first eye, pNAION was induced in the contralateral eye, and ranibizumab (J1, O1) or vehicle (A1, S1) administered, using the same technique. Neither the individual who performed the induction nor the individual who performed the IVT injections was masked as to which substance was being injected; however, the individual who performed the injections did not participate in the subsequent assessments of the animals.

**Optical Coherence Tomography.** Optical coherence tomography was used to assess the thickness of the PRNFL and the total macular thickness. We used a Heidelberg Spectralis spectral-domain HRA + OCT (SD-OCT) instrument (Heidelberg Engineering, Heidelberg, Germany) with 5.4b-US software and equipped with an automated real time eye-tracking system (ART). Before imaging, each animal's pupils were dilated with topical 2.5% phenylephrine and 1.0% tropicamide. For assessment of the PRNFL, the circular scan mode was employed, which uses a circle measuring 3.5 mm in diameter. One hundred images were averaged. A minimum of three scans was obtained for each eye at the same location, following which manual segmentation was performed by the same investigator (NRM). After segmentation, the thickness of the PRNFL was averaged among the three scans and assessed using the global measurement. For total macular thickness, the posterior border of Bruch's membrane was used as the outer boundary. We obtained scans with 30 images averaged per frame, and spacing between images of 120 μm. At least two sets of measurements were obtained, and the set with the best quality was used for manual segmentation. Again, all manual segmentation was performed by the same investigator (NRM). After segmentation, the volume of the macular retina was determined using the 3-mm Early Treatment Diabetic Retinopathy Study (ETDRS) circle grid.

**Electrophysiology.** Pattern VEPs and pattern ERGs (PERG) were performed prior to induction and at 1 day, 1, 2 and 4 weeks post induction of pNAION, and several later times over a period of an additional 2 to 3 months. Ganzfeld ERGs were performed at baseline, at 1 day and 4 weeks post induction, and just prior to euthanasia. All recordings were performed with both of the animal's pupils dilated with topical 2.5% phenylephrine and 1.0% tropicamide.

Pattern ERG and VEP: we obtained simultaneous PERG and VEP recordings with the monkey in the prone position and a Burian-Allen bipolar contact lens electrode placed on the eye. Potentials were recorded from each eye separately. To record simultaneous VEP and PERG waveforms, we modified a Topcon

Investigative Ophthalmology & Visual Science

fundus camera (TOPCON Corporation, Tokyo, Japan) by inserting a 2-cm organic light-emitting diode (OLED) screen from a head-mounted display into the split-viewer pathway.[18] The input to the screen was an alternating (1.9 Hz) black-and-white checkerboard pattern having a luminance of 109 cd/m$^2$ at a nominal contrast of 100%, generated by a LKC UTAS visual diagnostic system (LKC Technologies, Inc., Gaithersburg, MD, USA). The location of the screen was adjusted so that it was conjugate to the plane of the animal's pupil. In this way, when the monkey's retina was in focus, the image of the checkerboard was in focus on the monkey's retina. The macula was positioned using an infrared light source and an infrared-sensitive charged-coupled device (CCD) camera to avoid bleaching visual pigment. The field size stimulated was 45°. A 32 × 32 matrix was used, producing a check size of 56′. At intervals during the testing, the position of the animal's eye was reassessed using the infrared camera, followed by a resting period of 5 to 7 minutes to reduce the effects of light exposure.

For VEP recordings, the active electrode (Oz) was placed above the inion in the midline over the shaved skull, the reference electrode was placed in the midline frontal position (Fz), and the ground electrode was placed on an arm using Grass gold surface electrodes and EC2 electrode paste (Grass Instruments, Warwick, RI, USA). Recordings were repeated at least 10 times per eye; 8 to 10 consistent recordings were averaged offline to produce a waveform, the parameters of which were used in comparative analyses. For analysis of PERGs, the amplitudes of P50 (N35 trough to P50 peak) and N95 (P50 peak to N95 trough) waves were measured.[19]

**Ganzfeld ERG.** Ganzfeld ERGs were performed following 30 minutes of dark adaptation. A Burian-Allen bipolar electrode was placed in each eye and a ground electrode placed on an arm. Responses were elicited following the ISCEV protocol.[20] High and low band-pass filters were set at 0.3 Hz and 500 Hz, respectively. Oscillatory potentials were extracted using software developed by Severns and Johnson et al.,[21] available in existing LKC software.

**Optic Nerve Vascular Imaging.** Clinical optic nerve vascular imaging was performed using fluorescein angiography (FA). Fluorescein angiography was performed at baseline, 1 day and at 1, 2, and 4 weeks post-pNAION induction by intravenously injecting 0.30 mL of 25% fluorescein dye (AK-Fluor; AMP; Akorn, Decatur, IL, USA). Retinal and ON angiograms were obtained using a Topcon fundus camera with a standard excitation filter transmitting blue-green light at 465 to 490 nm, the peak excitation range of fluorescein, and a barrier filter transmitting a narrow band of yellow at fluorescein's peak emission range of 520 to 530 nm.

**Tissue Collection and Preparation.** Animals were euthanized from 12 to 20 weeks after induction of the second eye. Following deep surgical plane anesthesia, they were given an intracardiac saline perfusion followed by perfusion with 4% paraformaldehyde in PBS (PF-PBS). Both eyes were then enucleated. Following enucleation and post fixation in PF-PBS, ON tissues were prepared for standard histology either by paraffin embedding (7-μm thick sections) or by cryoprotection in 30% sucrose and frozen section embedding (10-μm thick sections) in optical cutting temperature compound. All nerves were embedded on end. After removal of the anterior segment, globes were incised to form a Maltese cross pattern, with the macula in the center of one of the arms. Each arm was bisected longitudinally, with half the arm saved for paraffin embedding and the other half for frozen section. Paraffin-embedded retinal sections (7-μm thick) were dewaxed and evaluated by staining with hematoxylin and eosin (H&E).

For transmission electron microscopy (TEM), ON tissue was postfixed in glutaraldehyde-paraformaldehyde buffer. For each animal, the ONs were placed on end and divided into an equal number of pie-shaped sections, impregnated with uranyl acetate, and shadowed with osmium. Each section was then embedded on end in Araldite-Epon.

**Immunohistochemistry.** Paraffin sections 7-μm thick of the ON were dewaxed and rehydrated. Following boiling citrate buffer (pH 6.0)-antigen retrieval, the sections were blocked with 2% donkey serum and incubated with mouse monoclonal antibody to neurofilaments (SMI312: Sternberg Monoclonals, Lutherville, MD, USA) for intact axons, rabbit anti-human glial fibrillary acidic protein (GFAP; ab7262; Abcam, Cambridge, MA, USA) for glial scarring at 1:1000 dilution, rabbit anti-myelin basic protein (MBP; NB100-872; Novus International, Brussels, Belgium) for myelination and rabbit antibody to the ionized calcium channel IBA-1 (Wako Chemicals, Osaka, Japan) for inflammatory cells at 1:500 dilution overnight at 4°C. Slides then were washed and incubated with the appropriate fluorescent-labelled secondary donkey antibody (Jackson Immunoresearch, West Point, PA, USA) for 4 hours at room temperature, followed by extensive washing. Slides were mounted with aqueous mounting medium and examined at the appropriate wavelengths using an Olympus four-channel confocal microscope (Center Valley, PA, USA).

**Electron Microscopic Analysis and Axon Quantification.** Cross-sections 200-μm thick were prepared from each embedded ON section, floated onto copper mesh grids, and examined by TEM using a Tecnai FEI T12 electron microscope (FEI, Hillsboro, OR, USA). An individual blinded to the substance injected in the eye from which the ON was obtained generated all axon counts. Counts were performed stereologically using the same number of axon fields in the two eyes of each monkey, with the understanding that among normal adult macaques, the age-independent mean of ON axons is approximately 1,100,000, with a range of 785,532 to 1,280,474 and a mean difference of 0.6% (SD = 1.7%) between the two eyes.[22] The fields were imaged at ×2100 to yield 131 μm$^2$ fields from each ON.

## Results

Clinical examination revealed that all four animals had normal pupillary reactions to light stimulation prior to induction of pNAION. Assessment of the pupillary reactions to light stimulation after induction of pNAION revealed an ipsilateral relative afferent defect (RAPD). The RAPD persisted regardless of whether vehicle or ranibizumab was subsequently injected. After the second eye was induced, three animals showed either a persistent RAPD in the eye injected with ranibizumab (A1, S1) or no RAPD (O1). Although animal J1 developed an RAPD in the first eye in which pNAION was induced and then injected with vehicle, we considered the significance of the subsequent pupillary reactions to light in this animal unclear because of the development of significant macular hemorrhage after injection of each eye. In addition, in all four animals, the optic disc and peripapillary swelling were similar in both the ranibizumab-treated eye and the vehicle-injected eye (Fig. 1; Supplementary Figs. S1–S3).

Fluorescein angiography revealed that in one animal (A1), optic disc edema appeared to persist for a longer period of time in the ranibizumab-treated eye than in the vehicle-injected eye (Fig. 2); however, in the other three animals, there was no obvious different in severity or duration of optic disc edema (Supplementary Figs. S4–S6).

Both clinically and by SD-OCT, the animals showed a variable amount of both peripapillary intraretinal edema and peripapillary subretinal fluid that gradually resolved over

Investigative Ophthalmology & Visual Science

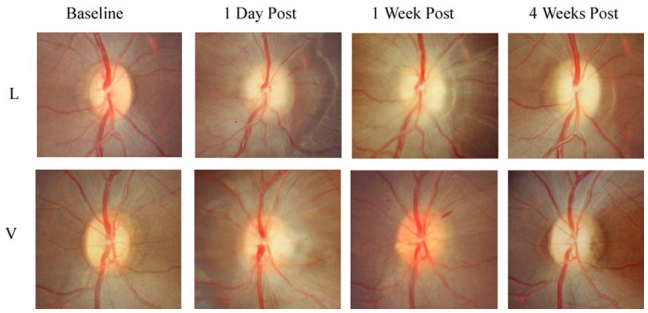


FIGURE 1. Color photograph of the optic discs of the right (*above*) and left (*below*) eyes in animal S1 after induction of pNAION followed within 15 minutes by a single intravitreal injection of either 0.05 mL of ranibizumab (L) (right eye, total dose = 0.5 mg) or 0.05 mL of vehicle (V) (left eye). Note that there is no obvious difference in the degree of swelling of the right and left optic discs at both 1 day and 1 week post injection, and that at 4 weeks post injection, there is no difference between the two eyes in the severity of optic disc and peripapillary retinal nerve fiber layer atrophy.

approximately 2 weeks. In all of the animals, the thickness of the PRNFL as assessed by SD-OCT was markedly increased at post induction day 1, was further increased at 1 week post induction, and then gradually thinned thereafter. The rate of increase of the PRNFL thickness as well as the rate of thinning was identical in the two eyes of all four animals. In addition, in all animals, both the 4-week post induction assessment and the final assessment prior to euthanasia revealed no difference in thickness of the PRNFL between the eye injected with ranibizumab and the eye injected with vehicle (Fig. 3).

Three animals underwent quantification of macular edema using SD-OCT. There was no significant difference between the vehicle-injected and ranibizumab-treated eyes (Fig. 4). The fourth animal (J1) developed significant bilateral macular hemorrhages and, thus, the degree of macular edema could not be assessed in this animal.

With respect to electrophysiological testing, none of the three animals assessed showed better VEP amplitudes in the ranibizumab-treated eye than in the vehicle-injected eye. Indeed, animal A1 showed persistently better amplitudes in the vehicle-injected eye than in the ranibizumab-treated eye, whereas animals O1 and S1 showed the same degree of reduction in the VEP amplitude at 4 weeks post induction (Fig. 5). Pattern ERG findings showed no consistent differences in either P50 or N95 amplitudes between vehicle-injected and ranibizumab-treated eyes of animals A1, O1, or S1 (data not shown). Again, the development of bilateral macular hemorrhages in animal J1 precluded electrophysiological testing in that animal.

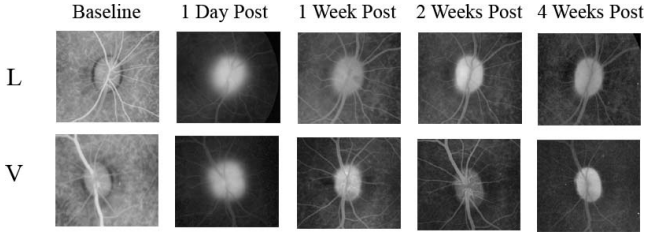


FIGURE 2. Fluorescein angiography of the right (*above*) and left (*below*) optic discs of animal A1 at similar times following fluorescein injection shows a similar amount of leakage of dye at 1 day and 1 week following rNAION induction and injection of either ranibizumab (L) or vehicle (V); however, at 2 weeks post induction and injection, there appears to be mild persistent leakage in the ranibizumab-injected eye compared with the eye injected with vehicle. At 4 weeks post induction and injection, the degree of staining is similar in both eyes.

## Histopathologic Findings

All four animals were euthanized at least 30 days after pNAION was induced in the second eye.

Both optic nerves were assessed by qualitatively and quantitatively. A representative analysis of a single animal (A1) is seen in Figure 5. Observation of H&E staining patterns (Figs. 6A, 6F) and axon loss of the total ON using SMI312 staining for intact axons (Figs. 6B, 6G), indicated that the ONs from both vehicle-injected and ranibizumab-treated eyes in all four animals had similar amounts of axon loss. Post ischemic demyelination was evident in areas of axon loss, as indicated by myelin colocalization with myelin basic protein (MBP; Figs. 6C–E). The penumbral regions revealed a diffuse, rather than sharp band of axon loss (Fig. 6D).

Staining for evidence of inflammation using IBA1 showed areas of persistent inflammation associated with increased GFAP signal in the region of axon loss (Figs. 6H–J). The regional GFAP increase was inversely related to the loss of expression of SMI312 (compare Figs. 6H–J with 6C–E). These findings are similar to those seen in the only histologically assessed clinical case of NAION.[23,24]

We confirmed the qualitative impressions made from observing the above staining patterns with a quantitative analysis of ON axon loss. The results of stereology confirmed the histologic findings in that in all four animals, despite a variation in the degree of overall damage among the animals, there was no significant difference in the number of remaining axons between the two eyes of three of the four animals (Table; Fig. 7). In the fourth animal (O1), 4% more axons were lost in the ON from vehicle-injected eye than in the ON from the eye treated with IVT Lucentis; however, these differences were substantiated by neither electrophysiology nor OCT.

## DISCUSSION

In this study, we have correlated the full range of clinically available imaging and electrophysiological analyses with axon stereology in a nonhuman primate model of NAION. The close agreement among the different tests used to evaluate structure and function validated the use of any one of them to evaluate damage from NAION. We found that for all three animals in which a complete assessment could be completed, ranibizumab treatment, given immediately after induction of moderate-to-severe pNAION, did not reduce the amount of pNAION-associated damage compared with contralateral vehicle-injected control eyes, regardless of the severity of the stroke. Specifically, there was no difference in the degree of optic disc swelling or in the degree or rate of its resolution by fundus photography, and there was no difference in the rate of severity of PRNFL thickness or macular edema by OCT imaging in vehicle-injected compared with ranibizumab-treated eyes, parameters that have been shown to correlate with visual acuity in human NAION.[25] In addition, there was no evidence of functional neuroprotection from ranibizumab as assessed by pupillary responses to light stimulation, VEP amplitude, or PERG N95 amplitude. The lack of functional ON preservation in ranibizumab-treated versus vehicle-injected eyes documented by electrophysiological findings was consistent with axon stereology. Thus, by all measures, a single IVT injection of ranibizumab conferred no neuroprotection following acute anterior ON ischemia when given immediately after induction. These results, which are consistent with those of Huang et al.[11] in their murine study of NAION and those of Rootman et al.[10]

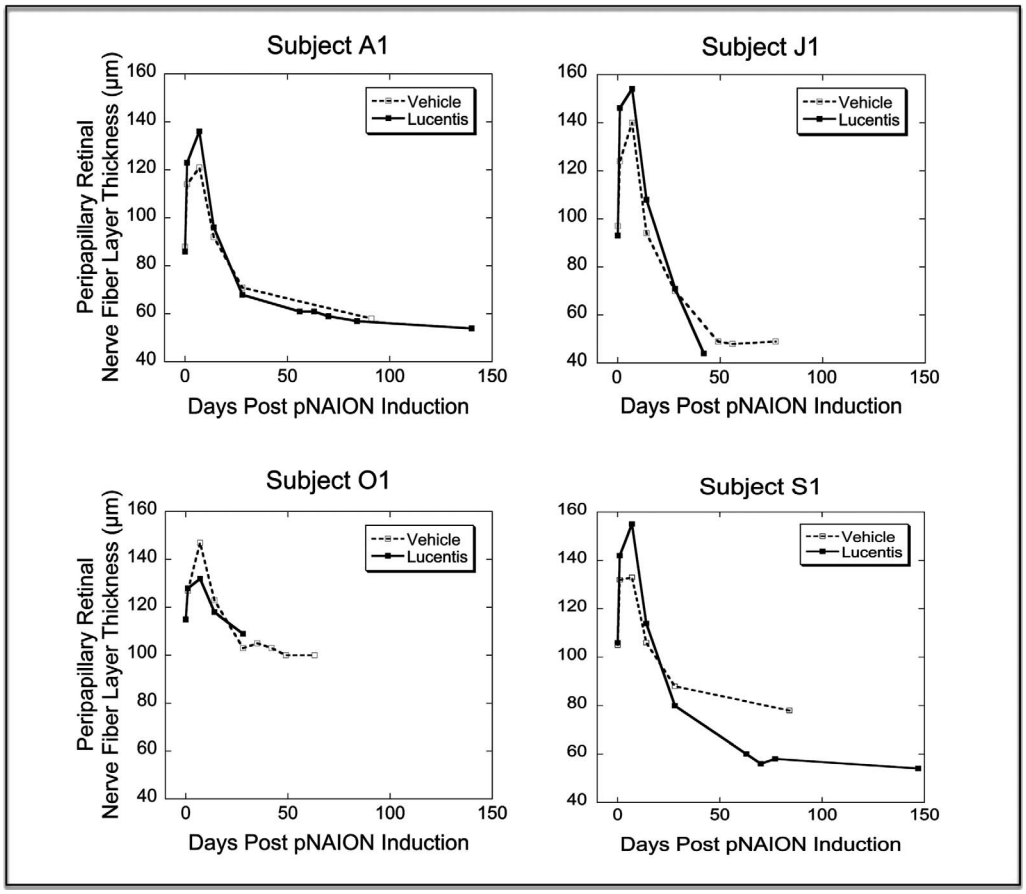


Figure 3. Peripapillary retinal nerve fiber layer (PRNFL) thickness at baseline and after induction of pNAION followed within 15 minutes by an intravitreal injection of either ranibizumab (Lucentis) or sterile saline (vehicle). Note that both the rate and the degree of thickening and subsequent thinning of the PRNFL are similar in the two eyes of all four animals (A1, O1, J1, S1).

in humans with spontaneous NAION, do not support its use in patients with moderate-to-severe NAION, those individuals most likely to warrant treatment.

The mechanism by which ranibizumab has been postulated to limit ON damage and improve ON function is not entirely clear, but it has been suggested that it reduces post ischemic edema, thereby reducing the damage caused by a secondary compartment syndrome.[23] In our animals, however, we could not detect any difference in the severity of optic disc or peripapillary retinal edema, the time course of edema resolution, or the ultimate thickness of the PRNFL and macula between eyes injected with ranibizumab and eyes injected with vehicle. Similarly, there were no differences in the relative amount of inflammation or post infarct demyelination when compared between the two eyes of each animal.

Because of the precious nature of primate resources, we wanted to maximize the information obtained from each individual animal and minimize the number of primates used

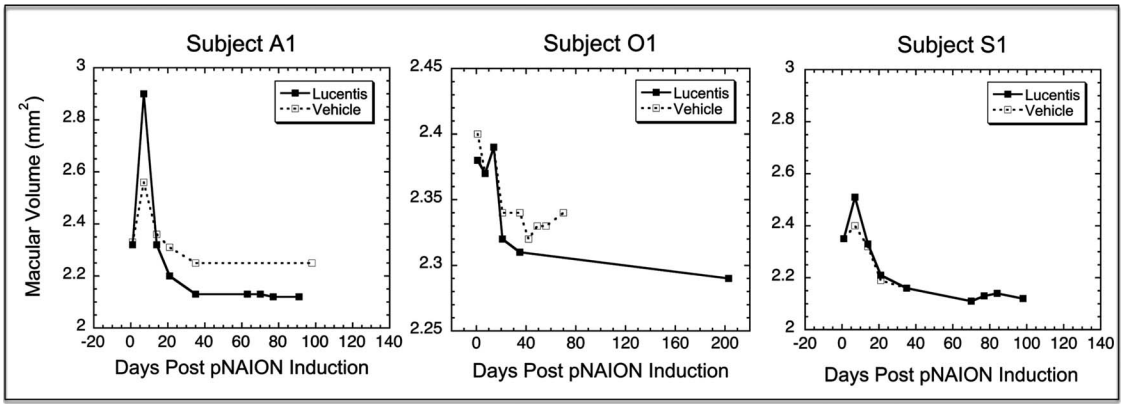


Figure 4. Macular thickness as assessed using SD-OCT. There is no significant difference between the vehicle-injected and the ranibizumab-treated eyes in the rate of development or severity of macular edema or the rate or severity of subsequent macular thinning in any of the three animals assessed (A1, O1, S1).

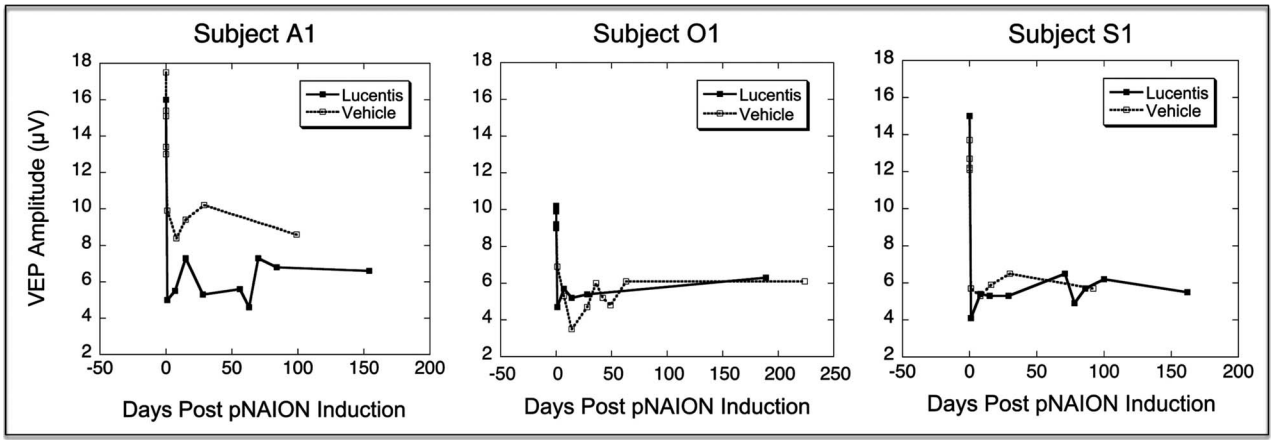


**Figure 5.** Visually evoked potential amplitudes in three animals. Note that in animal A1, the VEP amplitude is persistently higher in the vehicle-injected eye than in the ranibizumab-treated eye, whereas in animals O1 and S1, the VEP amplitudes in the two eyes are identical. There were no abnormalities in the ganzfeld ERG in any of the eyes injected with vehicle or ranibizumab (data not shown).

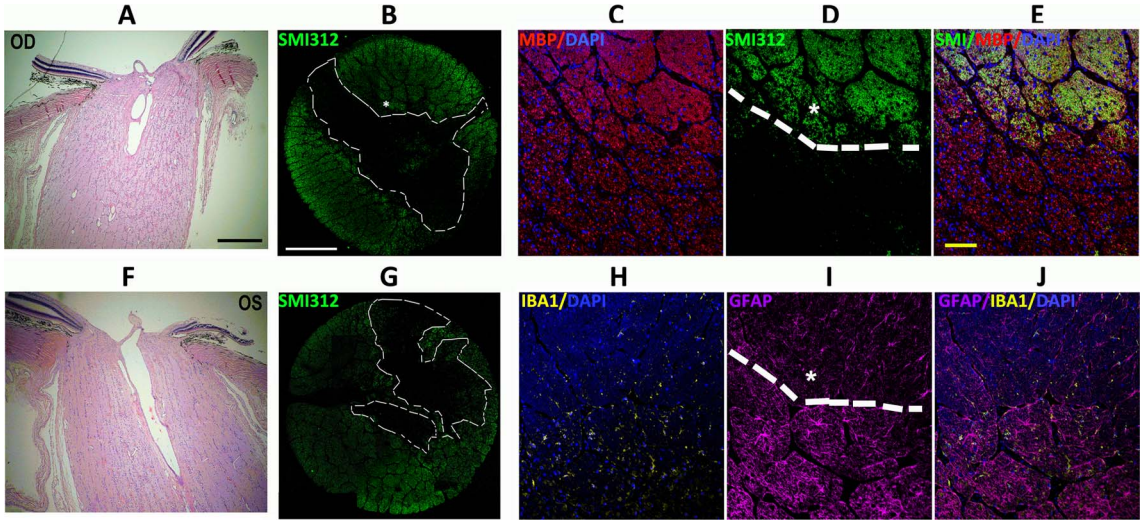


**Figure 6.** Histologic (**A**, **F**) and immunohistochemical (**B–E**, **G–H**) staining of the right (OD) and left (OS) optic nerves from animal A1. (**A**) and (**F**), H&E; (**B**) and (**G**), SMI312 immunostaining of the whole optic nerve. There is a similar amount of damage in the two nerves, as indicated by an increase in cellular prominence and thickened fibrovascular septae in (**A**, **F**), and absence of SMI312 staining in outlined areas in (**B**, **G**). (**C–E**): Confocal analysis of post-ischemic regional demyelination and axonal loss in the ON seen in the area of (**B**), indicated by an *asterisk*. Demyelination (indicated by a *dashed line*) is seen as a loss of signal in the inferior region ([**C**] and merged, [**E**], which is coupled to the loss of intact SMI312(+) axons (seen in [**D**] and merged, [**E**]). (**H–J**): Confocal analysis of post-ischemic cellular inflammation associated with scarring in the area indicated by an *asterisk* in (**G**). Section analyzed with IBA-1 (inflammatory cells) and GFAP (scarring). Relatively intact area is superior to the *dashed line*. Activated amoeboid inflammatory cells are scattered throughout the lower region in (**H**), and are associated with the greatest GFAP signal ([**I**] and merged, [**J**]).

**Table.** Optic Nerve Axon Counts Using Stereology

| | Animal | | | | | | | |
|---|---|---|---|---|---|---|---|---|
| | A1 | | J1 | | O1 | | S1 | |
| | Eye | | Eye | | Eye | | Eye | |
| | L | V | L | V | L | V | L | V |
| Total axons | 3180 | 2878 | 1180 | 1156 | 3375 | 3078 | 1016 | 1002 |
| Mean | 795.00 | 719.50 | 196.67 | 192.67 | 421.88 | 384.75 | 169.33 | 167.00 |
| SD | 279.86 | 210.45 | 160.05 | 105.86 | 53.74 | 54.58 | 49.00 | 58.36 |
| SEM | 139.93 | 105.23 | 65.34 | 42.96 | 19.0 | 19.3 | 20.00 | 23.82 |
| % Difference | 5% | | 2% | | 4.6% | | 0.7% | |
| *P* value | 0.16 | | 0.87 | | 0.006 | | 0.90 | |

Approximately 0.1%–0.2% of each nerve was counted using this method.

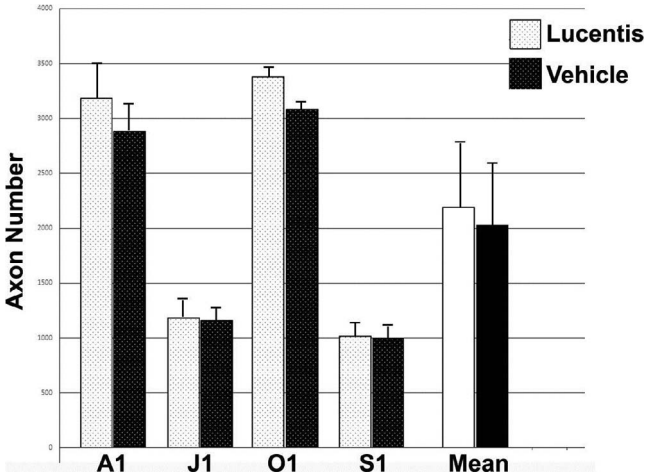


FIGURE 7. Stereological counts of axons in the two eyes of four adult monkeys obtained at least 30 days weeks after a single intravitreal injection of either ranibizumab or vehicle in the second eye. Although there were slightly more axons present in the eye injected with ranibizumab than in the contralateral eye injected with vehicle, only the difference in axon counts between the two eyes of animal O1 achieved statistical significance. The mean counts for the four animals were virtually identical.

for this study. We therefore assessed only four animals. Unfortunately, one of the animals developed severe macular hemorrhages and could not be assessed using all of our metrics. Nevertheless, the use of multiple functional tests (assessment of pupillary responses to light, VEP, PERG, ganzfeld ERG, in vivo imaging [IVFA, SD-OCT, fundus photos]) and, ultimately, histologic and immunohistochemical analyses of the eyes of the three animals that could be assessed completely at both baseline and post induction of pNAION enabled us to identify and compare ON ischemia-induced changes in retinal and ON structure and function in each eye with a high degree of sensitivity. Our ability to predictably and reproducibly generate a NAION-type defect is one of the great strengths of the current pNAION model. It should be emphasized again that although we induced visual impairment in all pNAION-induced eyes, none of the animals was blinded; all continued to see and respond appropriately. Judicious use of the pNAION model for analysis of potential clinical NAION treatments enabled us to use each animal as its own control. This approach can minimize variability and reduce the number of animals needed to analyze treatment efficacy, for future preclinical analyses.

## Acknowledgments

Supported by National Eye Institute Grant R01 EY019529 (Bethesda, MD, USA).

Disclosure: **N.R. Miller**, None; **M.A. Johnson**, None; **T. Nolan**, None; **Y. Guo**, None; **S.L. Bernstein**, None

## References

1. Arnold AC. Ischemic optic neuropathy. In Miller NR, Newman NJ, Biousse V, Kerrison JB, eds. *Walsh and Hoyt's Clinical Neuro-Ophthalmology*, 6th ed, Vol 1. Baltimore, MD: Lippincott-Williams & Wilkins; 2005:349–384.
2. Johnson LN, Arnold AC. Incidence of nonarteritic and arteritic anterior ischemic optic neuropathy: population-based study in the State of Missouri and Los Angeles County, California. *J Neuroophthalmol*. 1994;14:38–44.
3. Hattenhauer MG, Leavitt JA, Hodge DO, Grill R, Gray DT. Incidence of nonarteritic anterior ischemic optic neuropathy. *Am J Ophthalmol*. 1997;123:103–107.
4. Atkins EJ, Bruce BB, Newman NJ, Biousse V. Treatment of nonarteritic anterior ischemic optic neuropathy. *Surv Ophthalmol*. 2010;55:47–63.
5. Bernstein SL, Guo Y, Kelman SE, Flower RW, Johnson MA. Functional and cellular responses in a novel rodent model of anterior ischemic optic neuropathy. *Invest Ophthalmol Vis Sci*. 2003;44:4153–4162.
6. Goldenberg-Cohen N, Guo Y, Margolis F, Cohen Y, Miller NR, Bernstein SL. Oligodendrocyte dysfunction after induction of experimental anterior optic nerve ischemia. *Invest Ophthalmol Vis Sci*. 2005;46:2716–2725.
7. Bernstein SL, Guo Y, Slater BJ, Puche A, Kelman SE. Neuron stress and loss following rodent anterior ischemic optic neuropathy in double-reporter transgenic mice. *Invest Ophthalmol Vis Sci*. 2007;48:2304–2310.
8. Chen CS, Johnson MA, Flower RA, Slater BJ, Miller NR, Bernstein SL. A primate model of nonarteritic anterior ischemic optic neuropathy. *Invest Ophthalmol Vis Sci*. 2008; 49:2985–2992.
9. Bennett JL, Thomas S, Olson JL, Mandava N. Treatment of nonarteritic anterior ischemic optic neuropathy with intravitreal bevacizumab. *J Neuroophthalmol*. 2007;27:238–240.
10. Rootman D, Gill HS, Margolin EA. Intravitreal bevacizumab for the treatment of nonarteritic anterior ischemic optic neuropathy: a prospective trial. *Eye*. 2013;27:538–544.
11. Huang T-L, Chang C-H, Chang S-W, Lin K-H, Tsai R-K. Efficacy of intravitreal injections of antivascular endothelial growth factor agents in a rat model of anterior ischemic optic neuropathy. *Invest Ophthalmol Vis Sci*. 2015;56:2290–2296.
12. Mansour AM, Schwartz SG, Gregori NZ, et al. Insight into 8 patients with nonarteritic anterior ischemic optic neuropathy following anti-VEGF injections. *J Neuroophthalmol*. 2012;32: 193.
13. Mansour AM, Shahin M, Kofoed PK, Parodi MB, Shami M, Schwartz SG; for the Collaborative Anti-VEGF Ocular Vascular Complications Group. Insight into 144 patients with ocular vascular events during VEGF antagonist injections. *Clin Ophthalmol*. 2012;6:343–363.
14. Mäkelä K, Hartikainen K, Rorarius M, Jäntti V. Suppression of F-VEP during isoflurane-induced EEG suppression. *Electroencephalogr Clin Neurophysiol*. 1996;100:269–272.
15. Rosenfeld PJ, Schwartz SD, Blumenkranz MS, et al. Maximum tolerated dose of a humanized anti-vascular endothelial growth factor antibody fragment for treating neovascular age-related macular degeneration. *Ophthalmology*. 2006;112:1048–1053.
16. Maguire MG, Ying GS, Grunwald JE, Fine SL, Jaffe GJ; for the CATT Research Group, Martin DF. Ranibizumab and bevacizumab for neovascular age-related macular degeneration. *N Engl J Med*. 2011;364:1897–1908.
17. Giao-Grider Y, Hung L-F, Kee C, Ramamirtham R, Smith EL III. Normal ocular development in young rhesus monkeys (*Macaca mulatta*). *Vis Res*. 2007;47:1424–1444.
18. Johnson MA, Slater BJ, Miller NR, Bernstein SL, Flower RW. A simple integrated system for electrophysiologic recording in animals. *Doc Ophthalmol*. 2009;119:9–12.
19. Bach M, Halina M, Holder GE. Standard for pattern electroretinography: International Society for Clinical Electrophysiology of Vision. *Doc Ophthalmol*. 2000;101:11–18.
20. Marmor MF, Holder GE, Seeliger MW, Yamamoto S. Standard for clinical electroretinography. *Doc Ophthalmol*. 2004;108: 107–114.
21. Severns ML, Johnson MA, Bresnick GH. Methodological dependence of electroretinogram oscillatory potential amplitudes. *Doc Ophthalmol*. 1994;86:23–31.

22. Cull GA, Reynaud J, Wang L, Cioffi GA, Burgoyne CF, Fortune B. Relationship between orbital optic nerve axons counts and retinal nerve fiber layer thickness measured by spectral domain optical coherence tomography. *Invest Ophthalmol Vis Sci*. 2012;53:7766–7773.
23. Tesser RA, Niendorf ER, Levin LA. The morphology of an infarct in nonarteritic anterior ischemic optic neuropathy. *Ophthalmology*. 2003;110:2013–2035.
24. Salgado C, Vilson F, Miller NR, Bernstein SL. Cellular inflammation in nonarteritic anterior ischemic optic neuropathy and its primate model. *Arch Ophthalmol*. 2011;129:1583–1591.
25. Rebolleda G, Sánchez-Sánchez C, González-López JJ, Contreras I, Muñoz-Negrete FJ. Papillomacular bundle and inner retinal thicknesses correlate with visual acuity in nonarteritic anterior ischemic optic neuropathy. *Invest Ophthalmol Vis Sci*. 2015;56:682–695.

Investigative Ophthalmology & Visual Science